

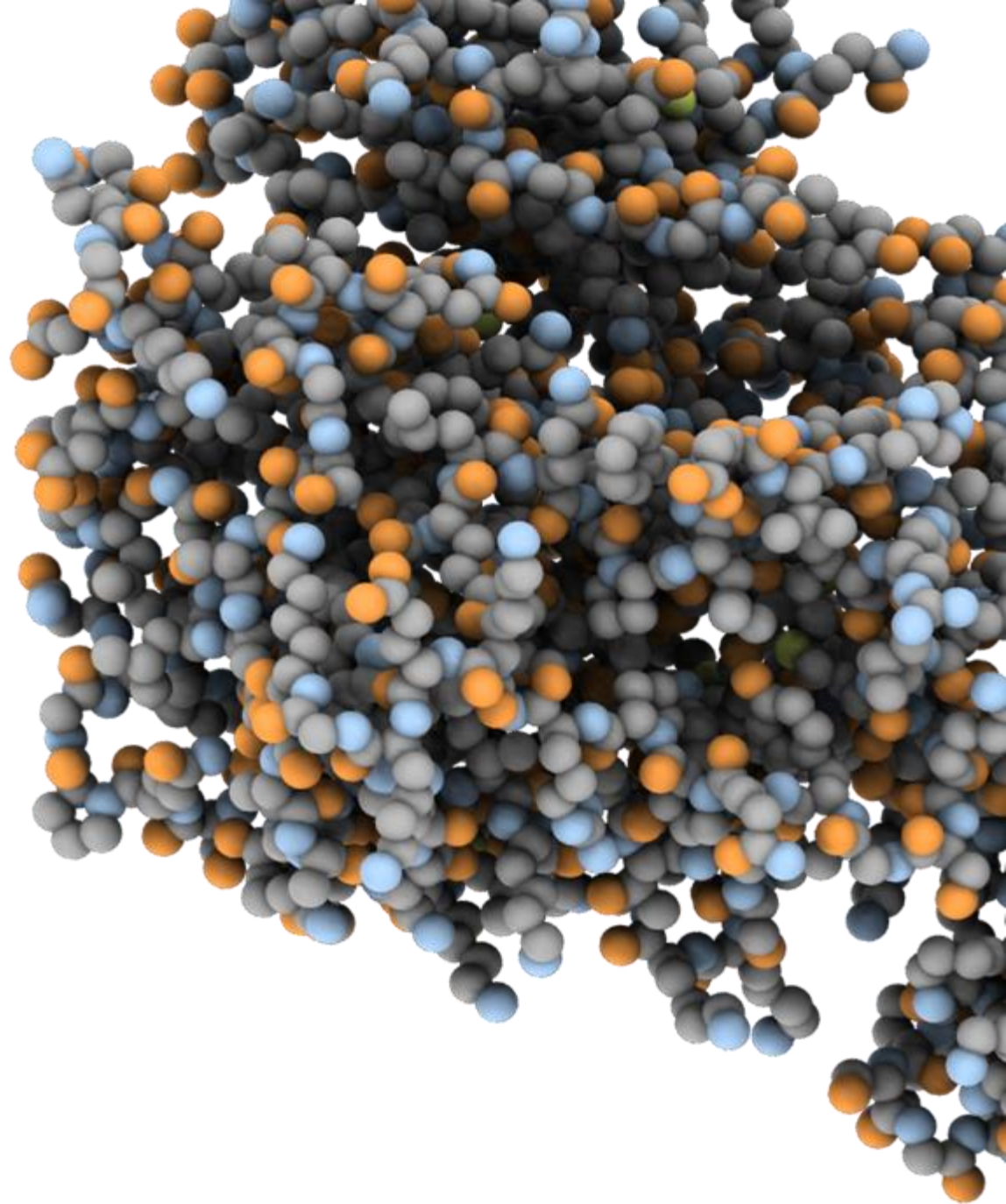


Discovery of NDI-101150, A Highly Potent and Selective HPK1 Inhibitor for the Treatment of Cancer, Through Structure-Based Drug Design

Neelu Kaila (on behalf of the HPK1 team)

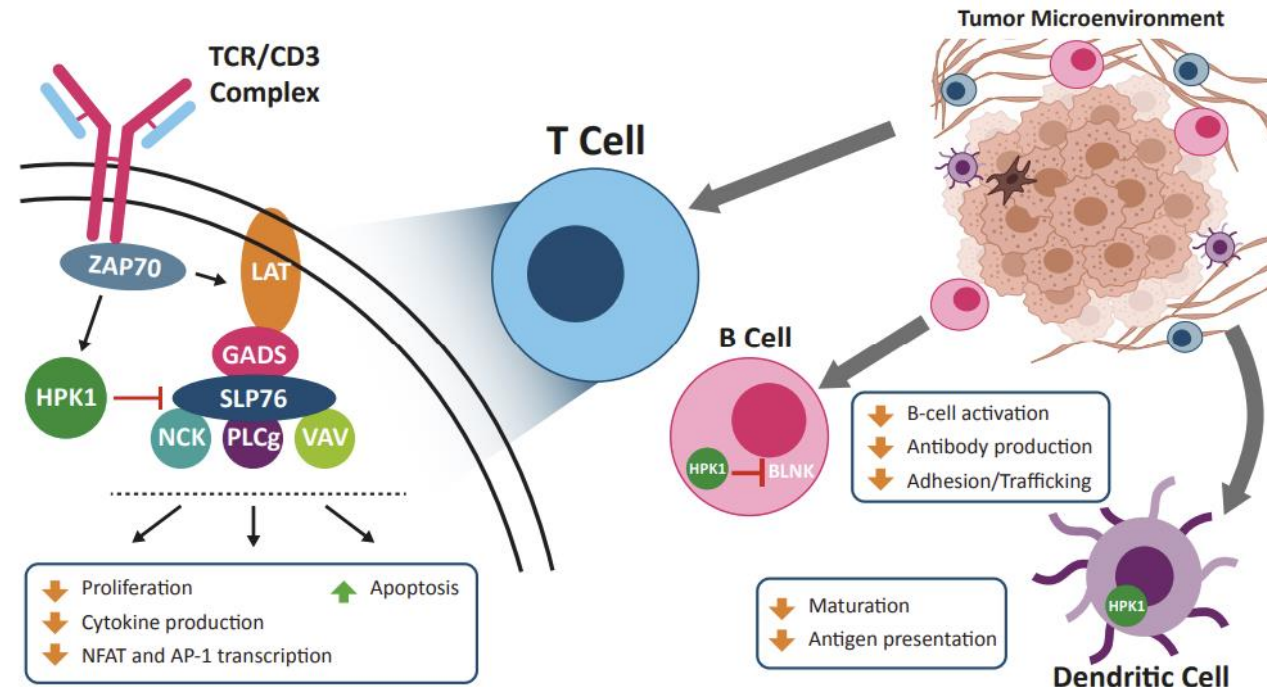
Nimbus Therapeutics

2024



Hematopoietic Progenitor Kinase 1 (HPK1, MAP4K1)

A Compelling Immuno-Oncology Therapeutic Target Due to Role in Broad Multi-Immune Activation

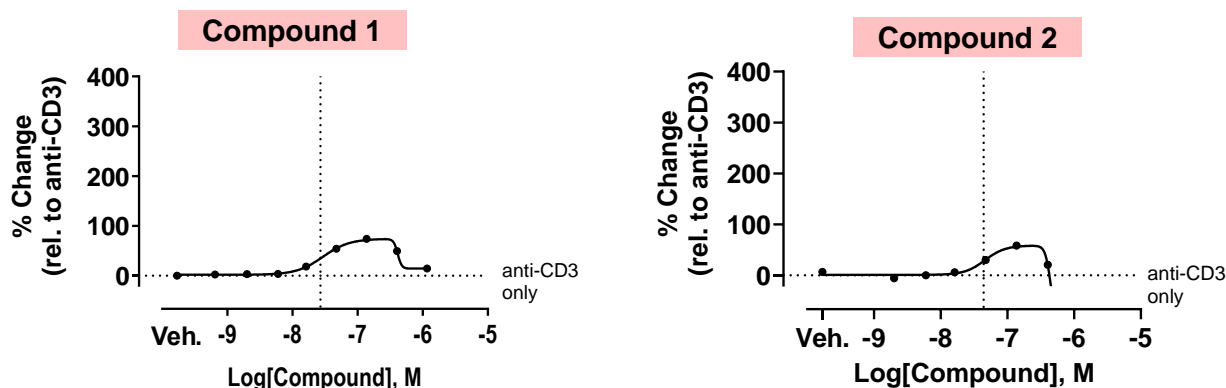


- Negative regulator of T cell, B cell, and dendritic cell-mediated immune response^{1,2}
- Expression is restricted to hematopoietic cells
- Genetically validated target
 - HPK1^{-/-} mice have enhanced anti-tumor T-cell response and are resistant to growth of Lewis lung carcinoma^{1,2}
 - HPK1 kinase-inactive-knock-in mice show impaired GL261 tumor growth, associated with increased T-cell infiltration^{1,2}
- The MAP4K family consists of 6 members with varied and compensatory roles in immune cell signalling and inflammation
- MAP4K1 and MAP4K4 are negative regulators and MAP4K3 (GLK) is a positive regulator of the T-cell activation
- **Key requirements for HPK1 inhibitor design is to get selectivity against**
 - **GLK and kinases involved in the propagation of TCR signalling, such as Src and other STE20-like family of kinases**

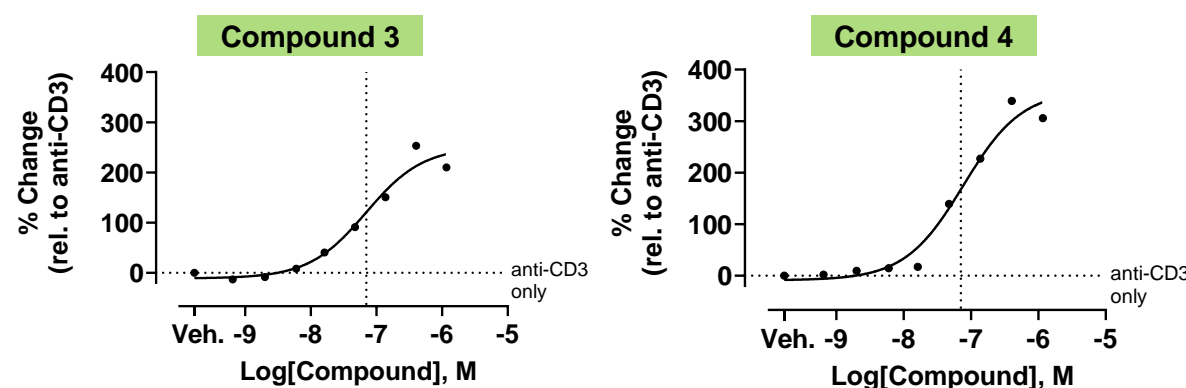
A High Degree of HPK1 Inhibitor Selectivity is Required for Cellular On-target Activity

IL-2 induction in primary mouse T cells: Compounds with superior GLK selectivity have improved functional activity compared to those with poor selectivity. **Potency alone is not enough to induce immune response you need GLK selectivity**

Potent HPK1 inhibitors with poor GLK selectivity



Potent HPK1 inhibitors with good GLK selectivity



Compound	Biochem HPK1 IC ₅₀ (nM) @ 1mM ATP	HPK1 cell IC ₅₀ (nM)	GLK Biochem selectivity (Fold vs HPK1 @ 1 mM ATP)
1	1.7	97	3
2	0.5	100	5
3	2	120	150
4	3	93	160

- EC₅₀s shift to the left (more potent) and the magnitude of IL-2 induction (peak response) increases with improved GLK selectivity

Origins of Nimbus HPK1 Chemical Matter

Virtual Screen

- 4 Receptor ensemble (3 HPK1 & 1 GLK) co-crystals
- Virtual library 11.5 M commercial compounds
- Filters used property space, Glide docking, Wscore
- 14 Hits Identified

Focus:

- SAR by catalog

Deprioritized due to poor potency of hits

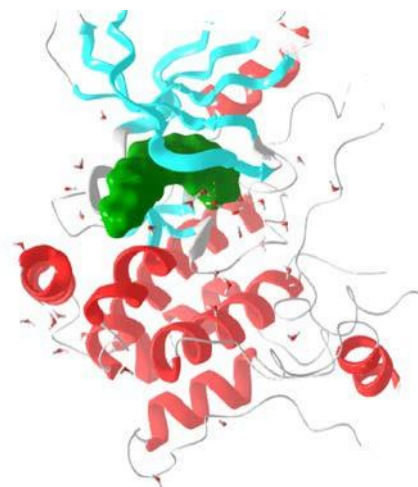
Literature-Based Hit Generation

- Identify known literature compounds with potent HPK1 inhibition - Good affinity, Poor selectivity

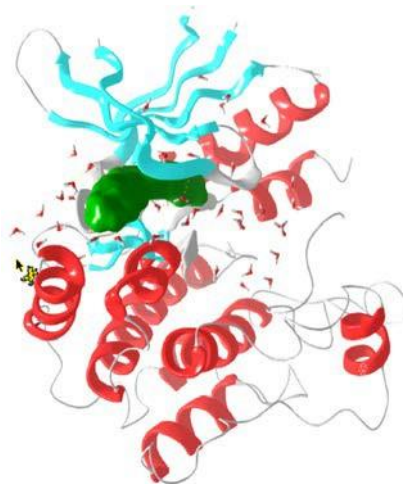
Focus:

- Obtain an HPK1 co-crystal to build selectivity

Deprioritized as we could not generate co-crystal with HPK1



Multiple HPK1/ GLK
Proprietary
Structures Obtained



Nimbus Library Hit

- Excellent affinity
- Poor Selectivity
- FEP/SBDD enabled. Multiple high resolution structures obtained

Focus:

- Improve selectivity
- Further ADME Profiling

Deprioritized in favor of the lead series due to moderate selectivity

Knowledge-Based Hit Generation

- Good affinity & selectivity
- FEP/SBDD enabled
- Lead Series

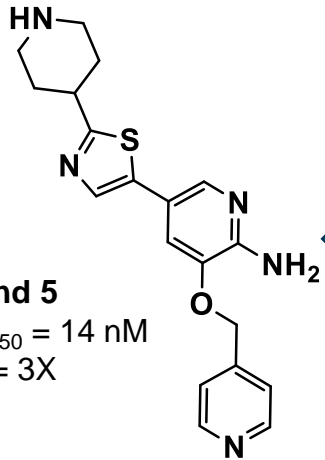
Focus:

- ADME Optimization

Prioritized due to excellent selectivity against GLK

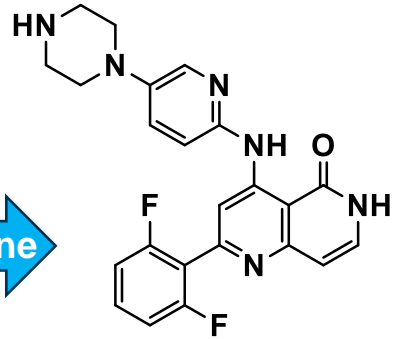
Knowledge Based Hit Generation

Literature

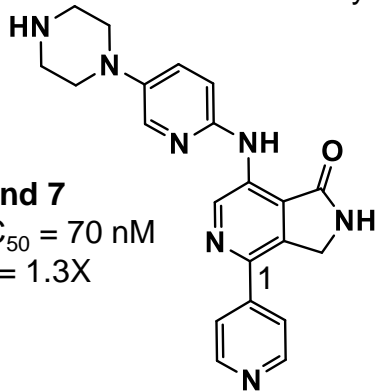


Compound 5
*HPK1 IC₅₀ = 14 nM
GLK Sel = 3X
Tyk2 NA

Nimbus Hit

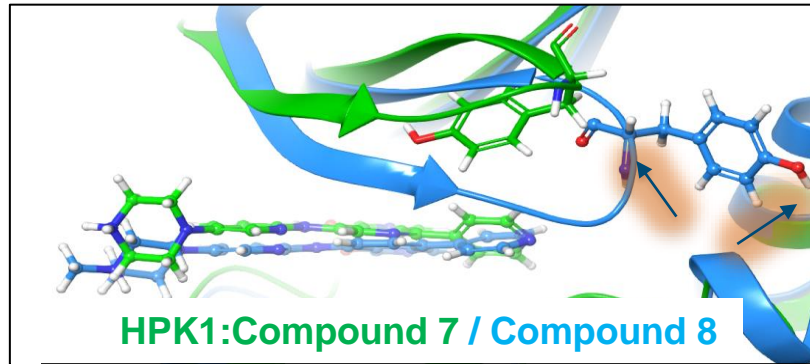


Compound 6
*HPK1 IC₅₀ = 4 nM
GLK Sel = 0.17X
Tyk2 Sel = 0.14X



Compound 7
*HPK1 IC₅₀ = 70 nM
GLK Sel = 1.3X
Tyk2 NA

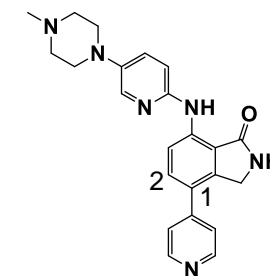
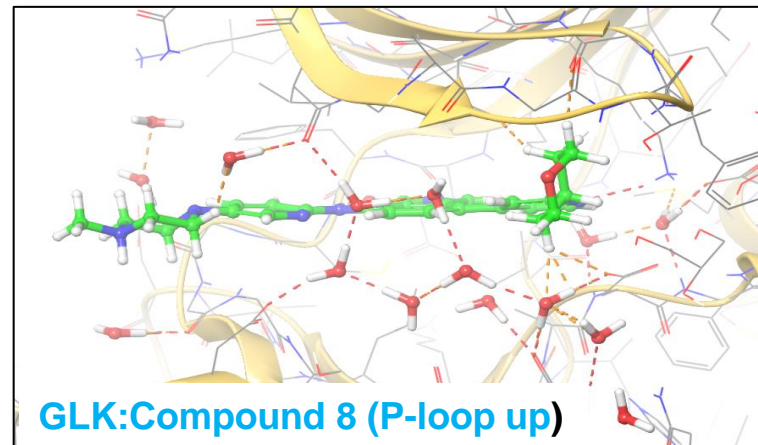
New series (aza isoindolinone) identified



Goal: Overlap of Tyr with C-1 substituent to improve HPK1 potency

P-Loop conformation affects orientation of identical residues

- Tyr 27 away from binding pocket in GLK: **Compound 8**
- Tyr 28 in binding pocket in HPK1:1 **Compound 7**



Compound 8
*HPK1 IC₅₀ = 98 nM
GLK Sel = 1.4X
Tyk2 NA

Goal: Break the water network to improve selectivity against GLK

- P-loop interacts directly with water network
- GLK structures show highly defined network near C1/C2 vectors



Significant Conformational Flexibility Observed in HPK1 and GLK X-ray Structures

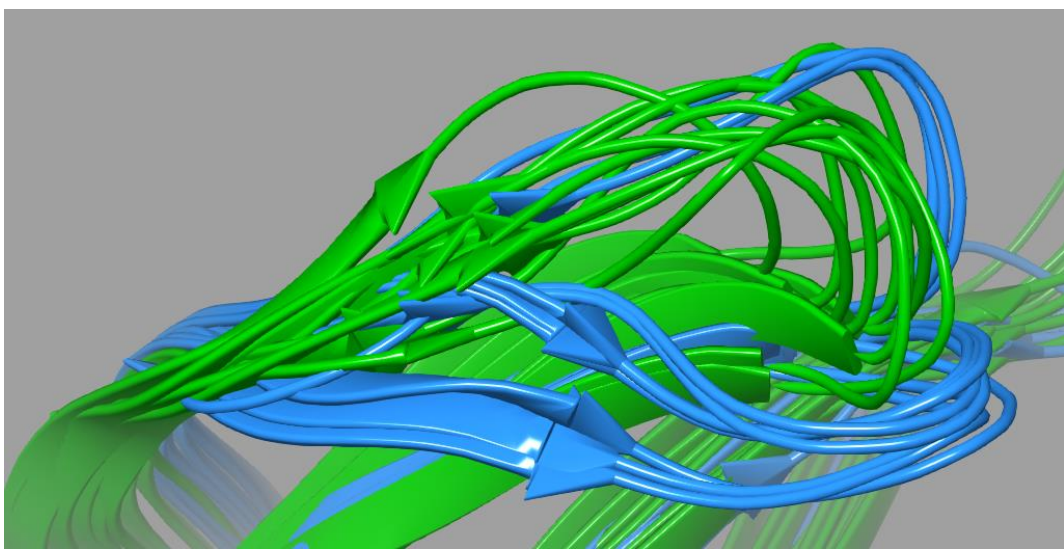
HPK1
13 Co-crystals (2 constructs)
C-Helix, activation and P-loops
take on a wide range of
conformations

GLK
31 Co-structures (5 constructs)
Soakable system
GLK P-loop alternates between
two positions

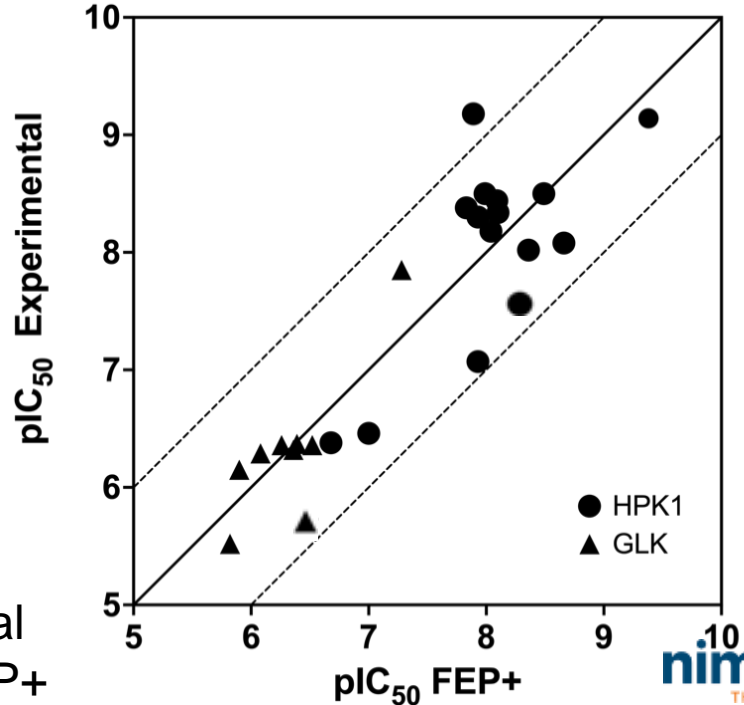
Flexibility of the P-loop creates challenges and opportunities

- Due to the dynamic nature of the P-loop use of FEP+ to increase potency and selectivity was challenging
- Enhanced flexibility of HPK1 provided a path to selectivity

Overlay of **HPK1 P-loop** and **GLK P-loop** from co-crystals with different ligands

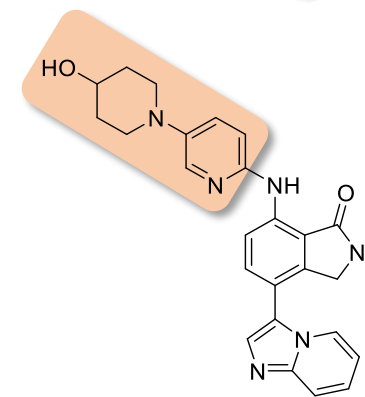
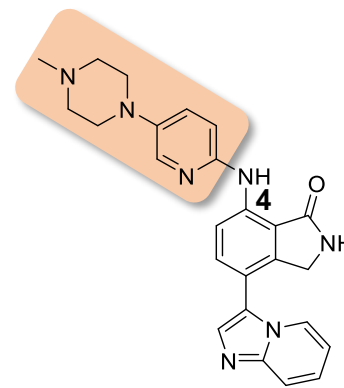
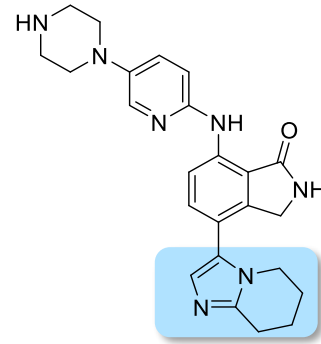
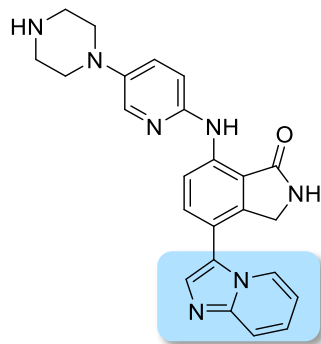
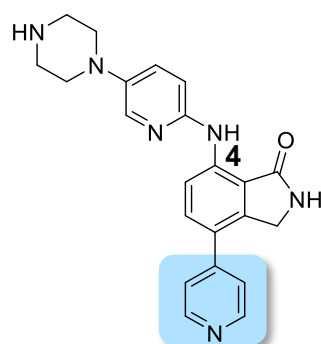


Prospective FEP+ predictions for HPK1 and GLK plotted against experimental



High-resolution ligand bound crystal structures facilitated the use of FEP+

Identification of Potent and Selective Bicyclic Series - Target Interaction with Tyr28



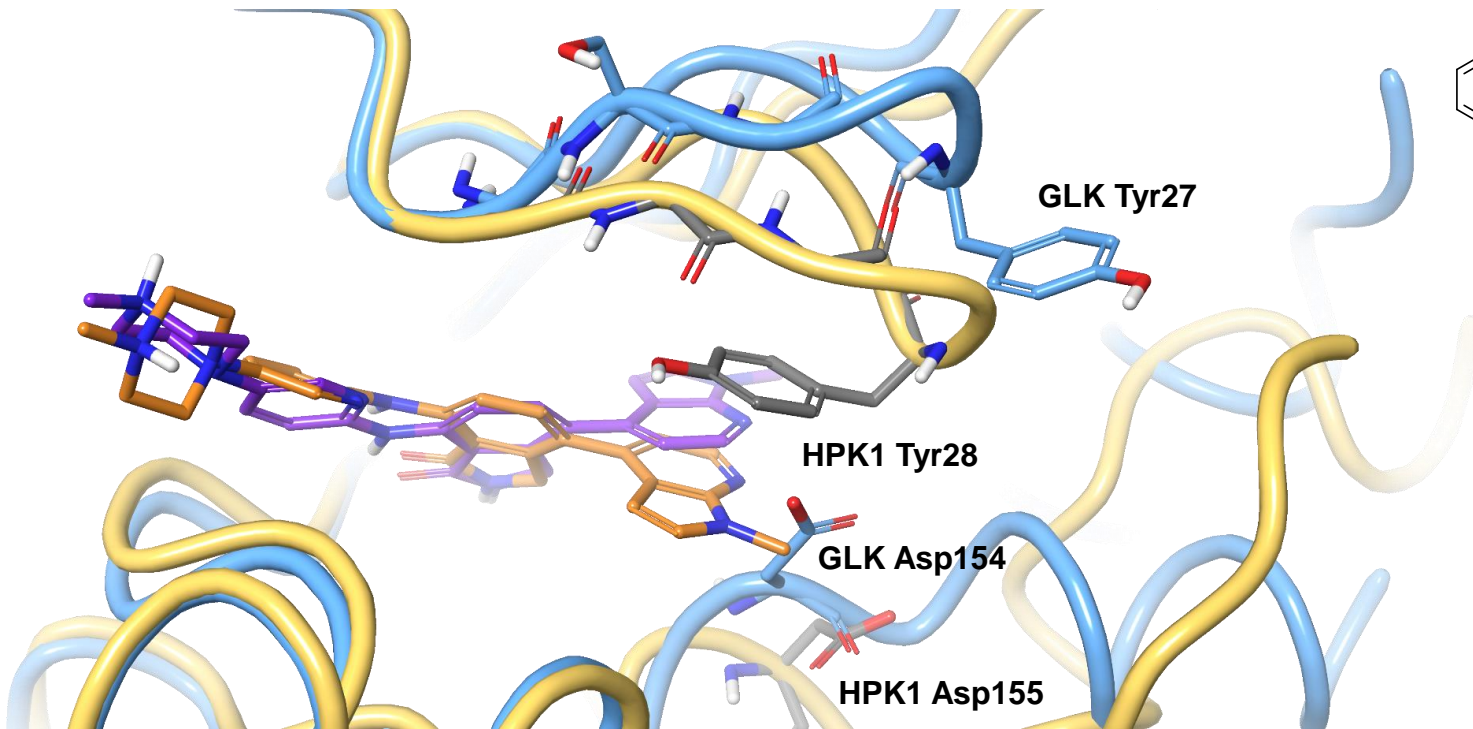
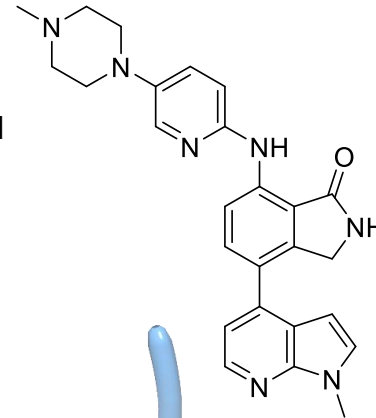
Assay	9	10	11	12	13
HPK1 ^a IC ₅₀ (nM)	43	1.8	15	0.8	2.6
GLK Selectivity ^b	1	26	21	74	46
Caco-2 P _{app, A-B} ^c / ER	5.7 / 14	0.6 / 92	0.4 / 29	26 / 2.8	--
AChE IC ₅₀ (nM)	--	--	--	26	>10,000

^aBiochemical potency at 1 mM ATP; ^b1 mM ATP; ^c10⁻⁶ cm/s

- Replacement of monocyclic pyridine with bicyclic aromatic rings improved HPK1 potency and selectivity against GLK
- Cross-screening identified acetyl choline esterase (AChE) inhibition as a significant liability for the C-4 piperazine series.
 - Compound **12** exhibited human AChE IC₅₀ of 26 nM
- Docking in a AChE literature structure showed that piperazine might be making a cation-π interaction with Trp86
 - Replacement of the basic piperazine compound **13** removed AChE inhibition (IC₅₀ > 10,000 nM)

Structural Basis for GLK Selectivity

Compound 14
Caliper 1 mM ATP
HPK1 IC₅₀ = 1.4 nM
GLK IC₅₀ = 84 nM
Selectivity = 60x



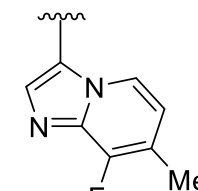
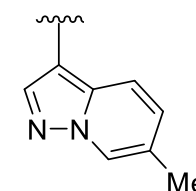
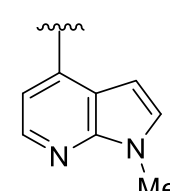
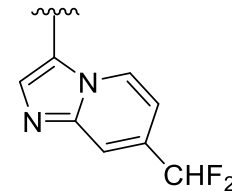
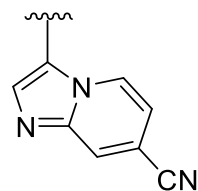
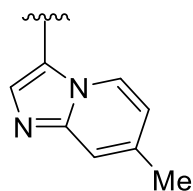
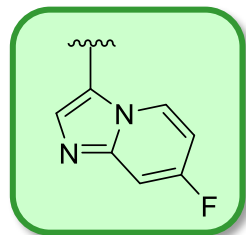
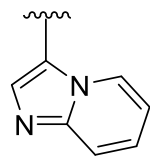
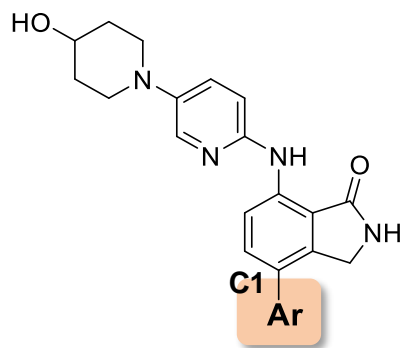
P-Loop confirmation affects orientation of identical residues Tyr 28 (HPK1 in the pocket) versus Tyr 27 (GLK away from pocket)
Gly-Gly-Gly HPK1 P-loop motif gives added flexibility over GLK with Gly-Ser-Gly

Flexibility of HPK1 P-loop allows Tyr28 π - π interaction with bicyclic Tyr27 for GLK is orientated away from the pocket and no interactions are present with 14

Conventional DFG Asp position as observed in GLK not compatible with ligand out orientation and needs to move for HPK1

HPK1 with bound Compound 14 (yellow ribbon, orange ligand)
GLK with bound Compound 14 (blue ribbon, purple ligand)

Identification of Potent and Selective C-1 Aryl Substituent

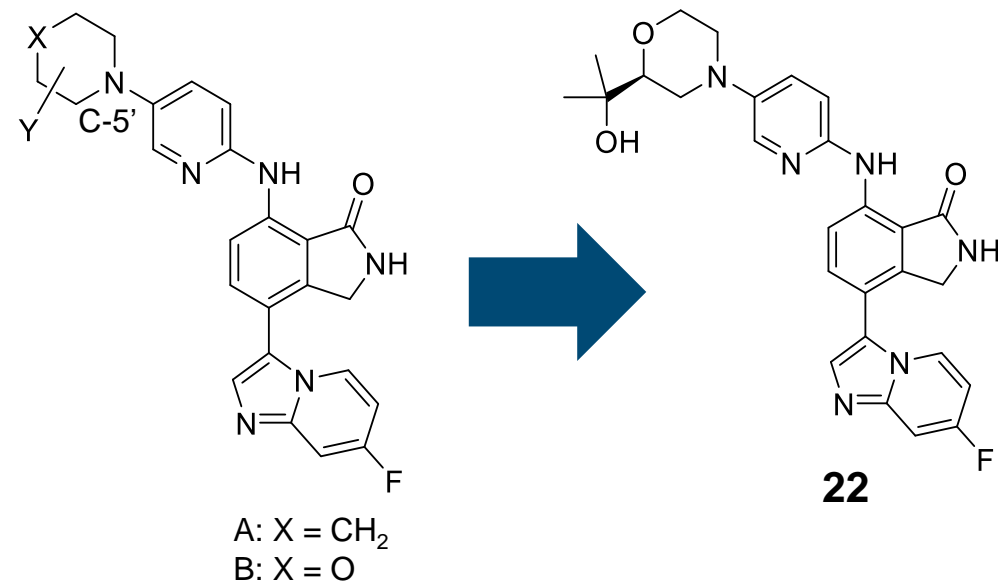
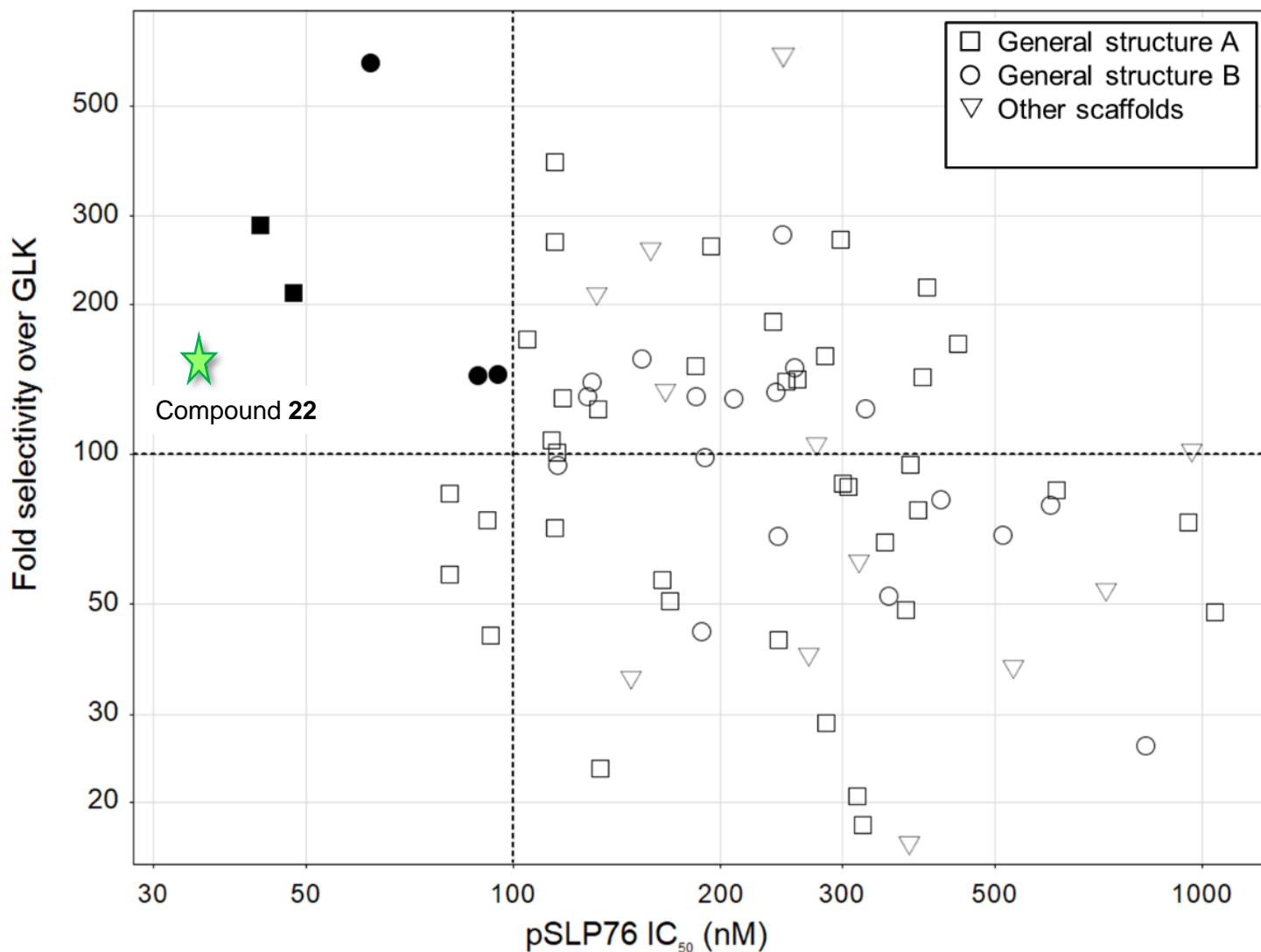


Assay	13	15	16	17	18	19	20	21
HPK1 ^a IC ₅₀ (nM)	2.6	4.2	1.8	0.7	3.6	2.2	0.9	0.5
GLK Selectivity ^b	46	127	175	439	269	91	180	152
Cell pSLP76 IC ₅₀ (nM)	116	101	1800	225	204	218	56	46
hPPB fu (%)	1.8	1.5	<1	<1	<1	<1	<1	<1

^aBiochemical potency at 1 mM ATP; ^b1 mM ATP

- Compounds are active in cell-based pSLP76 assay
- High plasma protein binding: few compounds have a measurable free fraction in human PPB measurements
- Compound **15** had the best balance of physical properties, GLK selectivity and cellular potency
 - At 75 mpk, it showed only 4 hours coverage of pSLP76 IC₅₀

Identification of Potent and Selective Solvent Facing C-5' Substituent

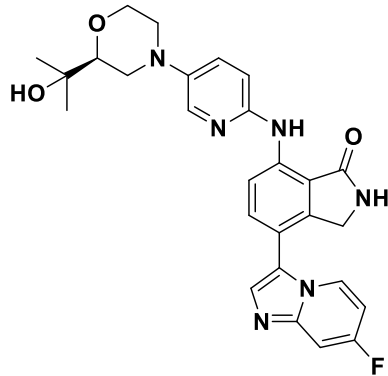


Compound **22** identified as a lead compound

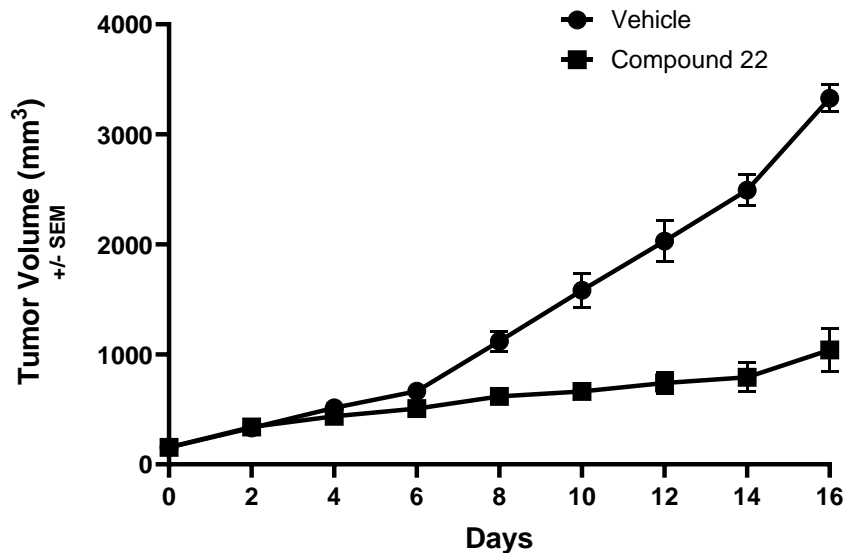
- >100-fold selectivity against GLK and good potency in biochemical and pSLP76 assay
- In a mouse PO PK study at 75 mpk showed 24 hour coverage of pSLP76 IC₅₀

Early Frontrunner (Compound 22) Exhibited Suboptimal Predicted Human PK

Potent and selective HPK1 inhibitor

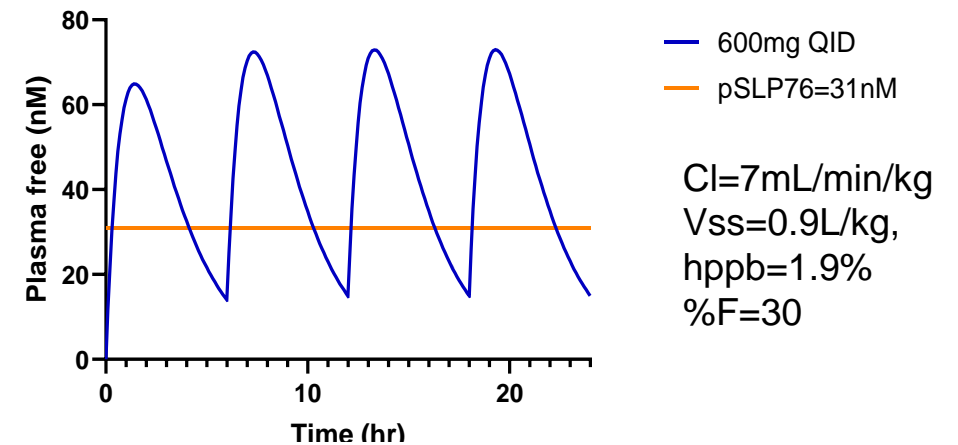


Assay	Compound 22	Assay	Compound 22
HPK1 IC ₅₀ 1mM ATP	0.7 nM	MDCK (x10 ⁻⁶ cm/s) A-B / EER	52 / 15
HPK1 pSLP76 IC ₅₀	31 nM	Kinetic solubility (FeSSIF)	>200 μM
Selectivity assessment (fold selectivity @ [1 mM ATP])		hHeps (mL/min/Kg) Clpred	< 8
GCK / MAP4K2	600	Mouse Cl _{obs} (mL/min/Kg) (mHeps)	11 (36)
GLK / MAP4K3	130	Rat Cl _{obs} (mL/min/Kg) (rHeps)	27 (26)
HGK / MAP4K4	2800	Dog Cl _{obs} (mL/min/Kg) (dHeps)	18 (17)
KHS / MAP4K5	100	hPPB (%)	98.1
MINK	2600	Rat V _{ss} (L/kg)	0.90
TNIK	500	Mouse V _{ss} (L/kg)	0.50
		Dog V _{ss} (L/kg)	1.6



- CT-26 syngeneic mouse model **22** dosed at 75 mpk PO QD
- Robust and statistically significant tumor growth inhibition(69%) observed with 16h coverage of pSLP76 IC₅₀

600mg QID Compound 22 needed for 16h coverage of pSLP76 IC₅₀



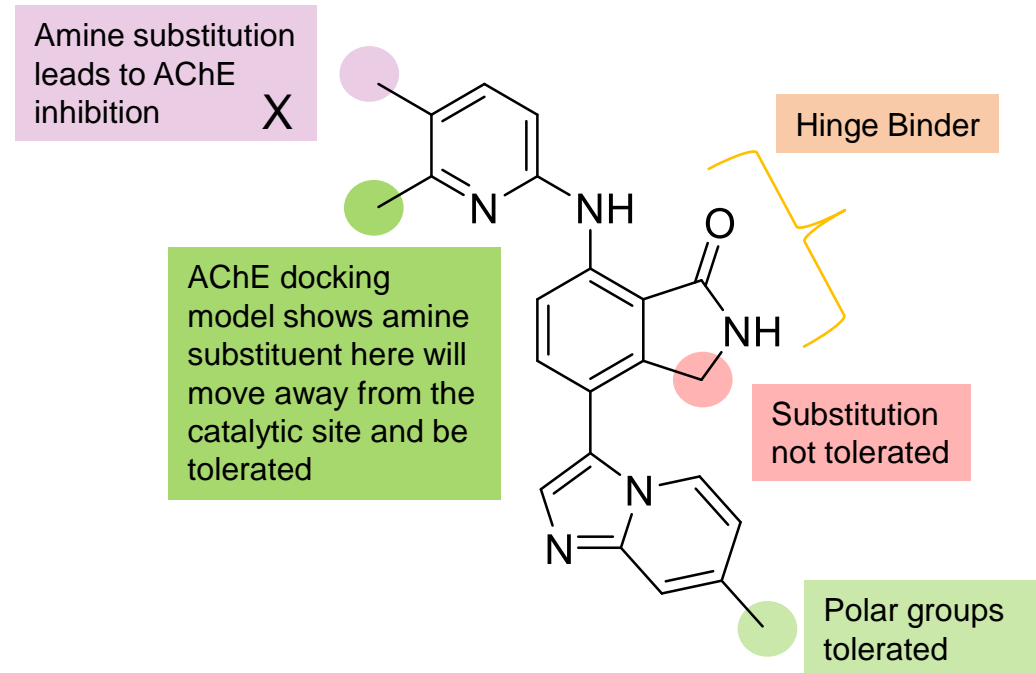
Predicted high dose high frequency in humans

Designing for Dose: Increased Volume of Distribution(Vd) and Half-life to Improve Predicted Human Dose

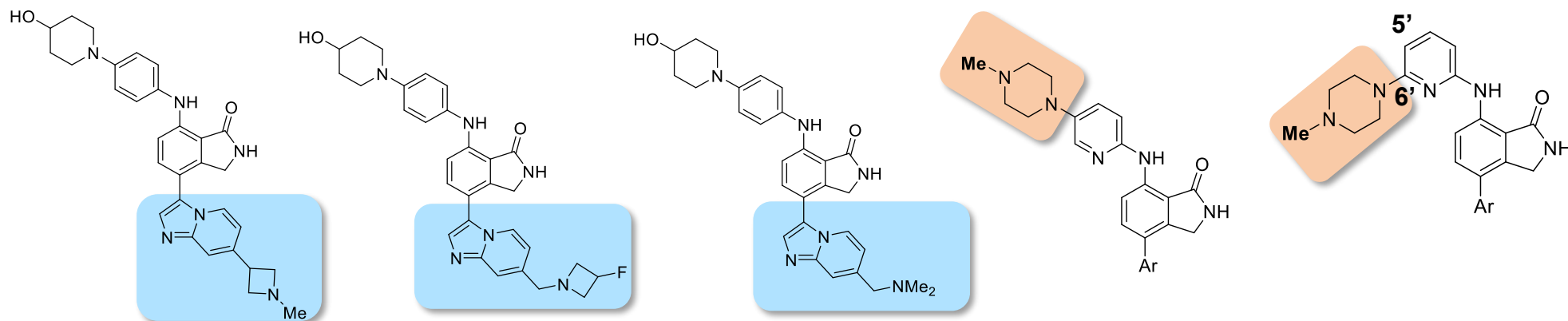
What parameters can we change to get reasonable predicted human dose?

Assay	Target Profile	Phys Props
HPK1 IC ₅₀ 1mM ATP (nM)	<1	
HPK1 cell IC ₅₀ (nM)	< 50	
GLK selectivity fold	> 100	
pK _A	> 7.5	Basic amine
hPPB (fu) %	measurable	cLog P < 3
HLM Cl (mL/min/kg)	≤ 12	
MDCK Permeability A-B (10 ⁻⁶ cm/s)	≥ 15	HBD ≤ 2
Volume of Distribution Vss L/kg	> 5	pKA > 7.5

Back to the drawing board



Medicinal Chemistry Strategy to \uparrow Vd and $T_{1/2}$: Add Basic Amine while Maintaining Potency and Selectivity



Assay	23	24	25	Series 26	Series 27
HPK1 ^a IC ₅₀ (nM)	2.4	336	174	<10	<10
GLK Selectivity ^b	498	--	--	>100	>100
AChE IC ₅₀ (nM)	1230	9950	2100	<50	>10000

^aBiochemical potency at 1 mM ATP; ^b1 mM ATP;

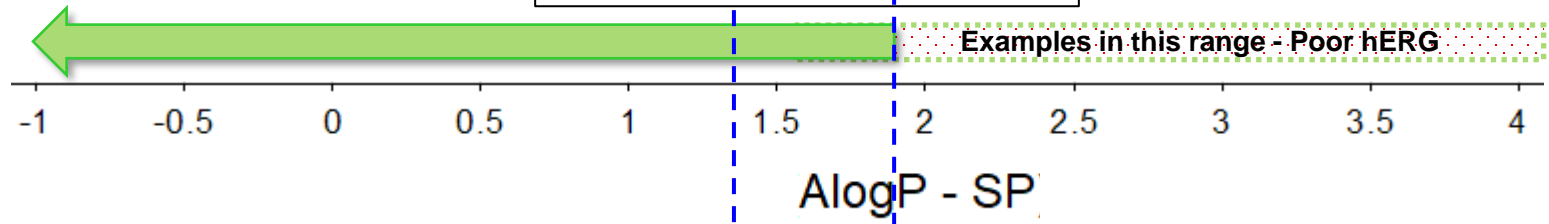
- Structural analysis suggested the imidazopyridine group may accommodate polarity – but potency and AChE selectivity was suboptimal (compounds **23-25**)
- HPK1 potency was retained when the amine pointed towards solvent (substitution of the pyridyl)
- The 6' substituted amine series **27** maintained HPK1 potency and selectivity against AChE
 - Further exploration at the 6' position was pursued



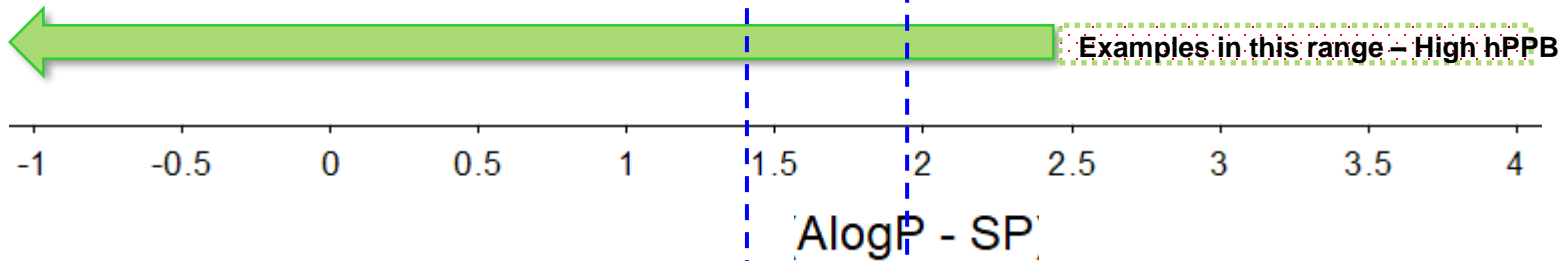
Optimizing Phys Props in the Basic Series - Impact of AlogP-SP on Different Parameters

AlogP-SP sweet spot
1.5 - 2

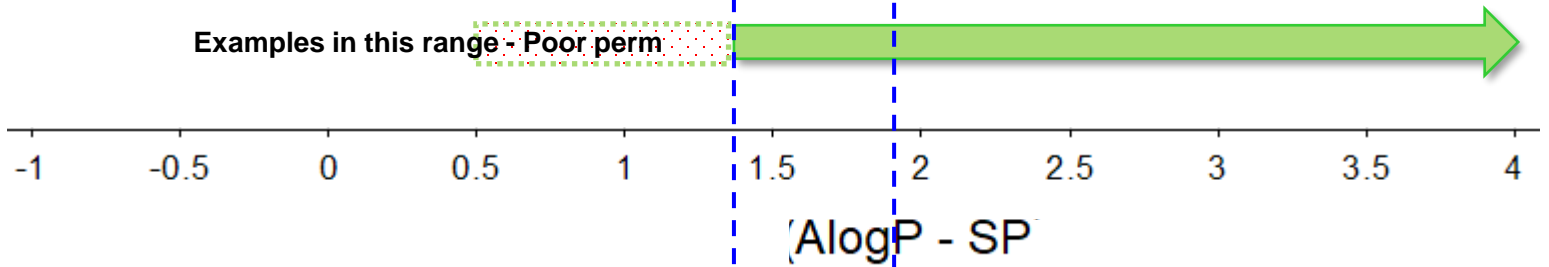
hERG IC₅₀ >5 μM



hPPB <99%



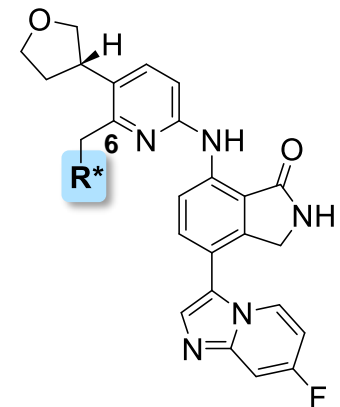
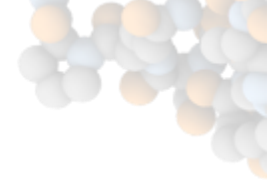
MDCK A to B >10
(10⁻⁶cm/s)



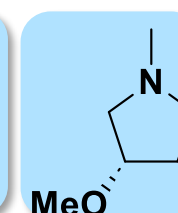
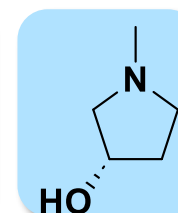
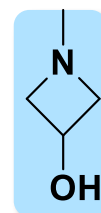
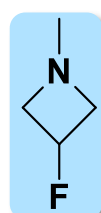
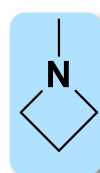
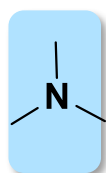
AlogP-SP* used to establish correlations to ADME properties. To achieve all 3 parameters need to be in sweet spot

* cLogP surrogate from Schrödinger

Identification of Development Candidate NDI-101150



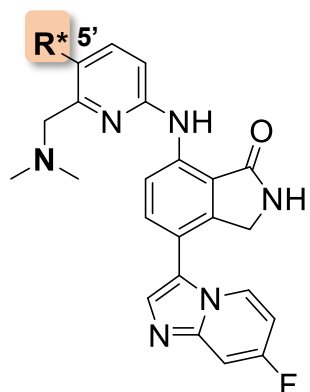
R* =



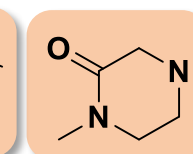
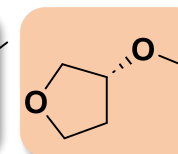
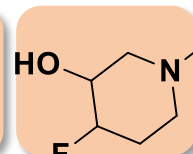
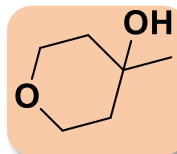
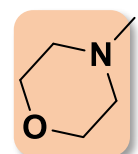
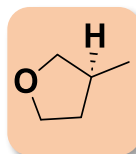
Assay	101150	28	29	30	31	32	33
HPK1 ^a /pSLP76 IC ₅₀ (nM)	0.7/42	1.3/154	0.6/134	0.8/300	0.4/18	0.8/151	0.7/32
GLK Selectivity ^b	377	523	518	288	258	265	429
MDCK WT P _{app, A-B} ^c	32	6	5	3	30	8	75
hHep Cl _{pred} (mL/min/kg)	8	10	14	8	18	14	17

- Dimethyl amine at C-6 shows best P_{app} and hHep Cl_{pred}

^aBiochemical potency at 1 mM ATP; ^b1 mM ATP; ^c10⁻⁶ cm/s; * stereochemistry arbitrarily assigned



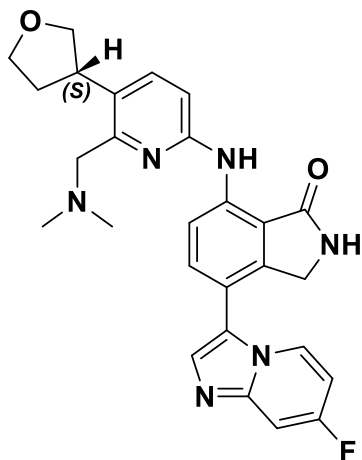
R* =



Assay	101150	34	35	36	37	38
HPK1 ^a /pSLP76 IC ₅₀ (nM)	0.7/42	0.9/88	0.9/114	2.1/74	0.5/176	1.1/540
GLK Selectivity ^b	377	469	613	256	1176	402
MDCK WT P _{app, A-B} ^c	32	19	8	8	9	
hHep Cl _{pred} (mL/min/kg)	8	<8	<9	<9	12	
hERG PC IC ₅₀ (nM)	2829	7218	12700	7712	1093	
Rat PK Vss (L/kg)/Cl (mL/min/kg)/F%	5/34/20	9/98/<1	17/82/4	23/73/<1		

- Low rat oral bioavailability could be driven by low permeability or high clearance

NDI-101150: Development Compound Profile



Assay	NDI-101150
Molecular Weight	486.5
Log P (measured)	2.6
Log D (measured)	2.0
pKa (measured)	8.9
Solubility (pH 7.4)	140 uM
MDCK P _{app} (x10 ⁻⁶ cm/s) / ER	32 / 0.7

HPK1 Assay	IC ₅₀ (nM)
Caliper @ 1 mM ATP	0.7
pSLP76	42
Kinase (Fold Selectivity)*	
GCK/MAP4K2	8000
GLK/MAP4K3	377
HGK/MAP4K4	10740
KHS/MAP4K5	489
MINK/MAP4K6	10740
TNIK/MAP4K7	1336
c-SRC	3630
FYN	3110
LCK	2143
SYK	20000
TYK2	30000

Assay	NDI-101150
Cyp Inhibition	1A2, 2B6, 3C8, 2C9, 2C19, 3A4M, 3A4T IC50 > 30 uM 2D6 IC50 = 17 uM No evidence of TDI at 50 uM
Cyp Induction	PXR activation assessed at 3/30uM no activation
hERG Manual PC IC ₅₀	2800 nM

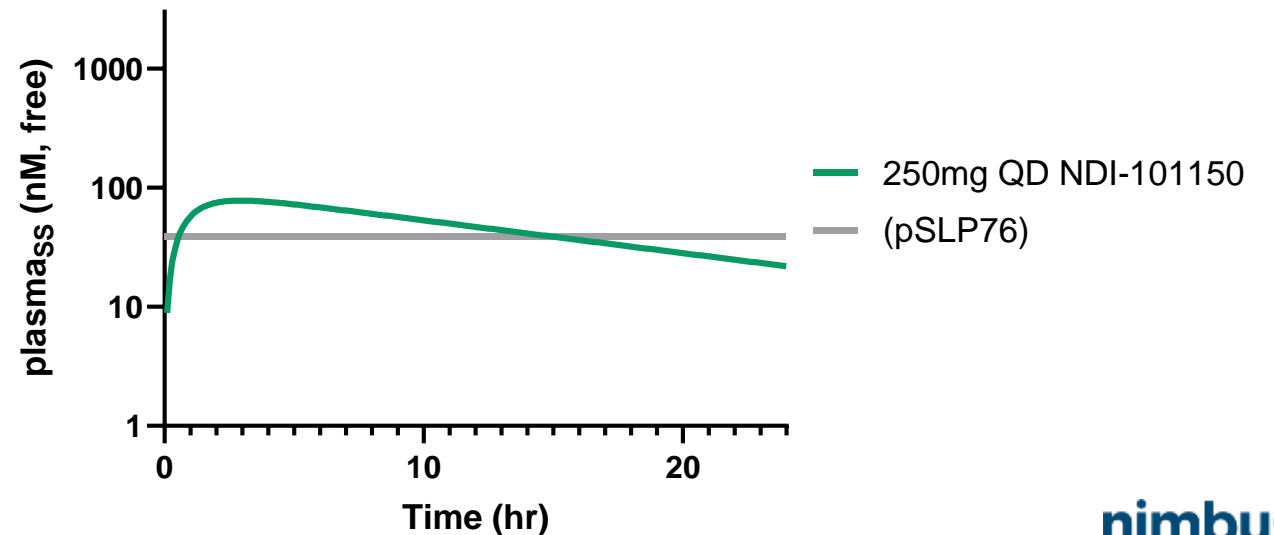
- In the GLP in vivo telemetry study in conscious monkeys no effects on cardiovascular function (HR, BP, ECG parameters)
- > 300-fold selectivity in 300+ kinase panel
- 4 hits in Eurofins panel. Secondary assays complete– no concerns.

NDI-101150: Suitable In Vivo Exposure and Clearance from Discovery PK Studies

Species	In vivo				In vitro		
	Cl (mL/min/kg)	V (L/kg)	Half life (hr)	F (%)	Microsomes (mL/min/kg)	Hepatocytes (mL/min/kg)	PPB (%)
Mouse	30	1.9	1.1	50	61	84	80
Rat	34	5.1	3	18-44	24	44	84
Monkey	16	3.3	6.1	14-24	36	22	87
Dog	43	13	6.8	33	26	24	73
Human	TBD	TBD	TBD	TBD	12-13	7	75

Early dose projection for 16 h pSLP76 coverage

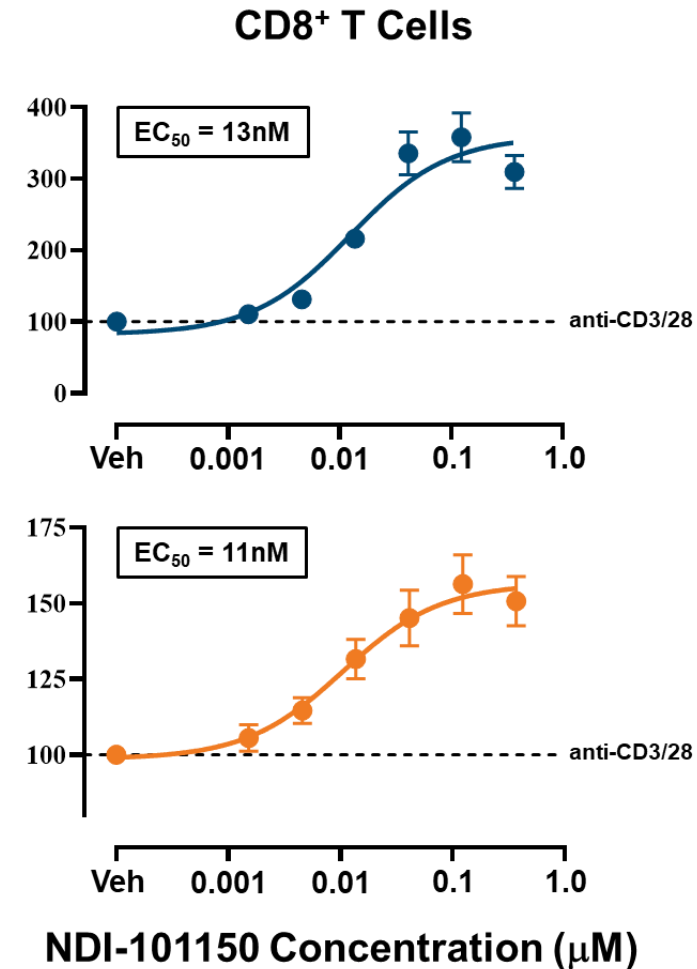
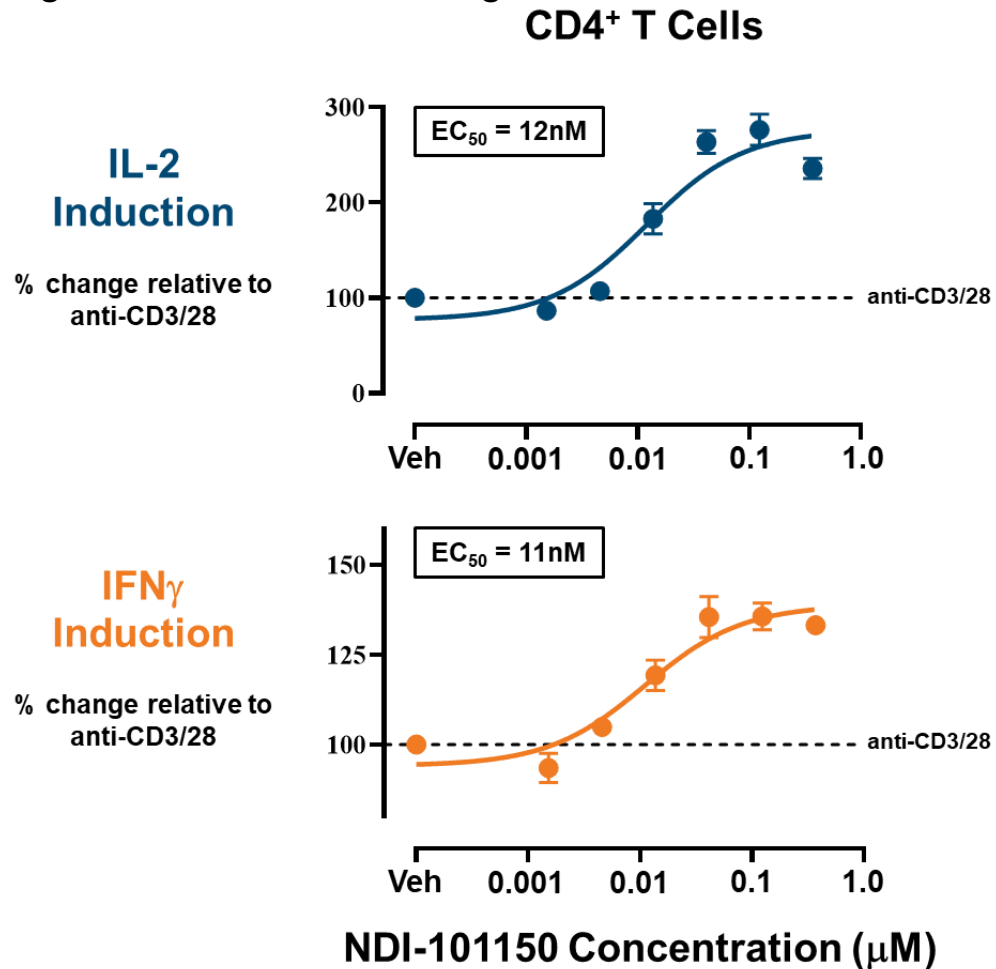
$V = 6 \text{ L/kg}$, $Cl = 7.2 \text{ mL/min/kg}$, $t_{1/2} = 11 \text{ h}$



Nimbus HPK1 Inhibitor NDI-101150 Preclinical Biology

NDI-101150 mediates activation of not only T cells, but also B cells and dendritic cells

- In human T cell activation assays, NDI-101150 was able to enhance the activation of both CD4+ and CD8+ T cells by increasing levels of IL-2 and IFN γ

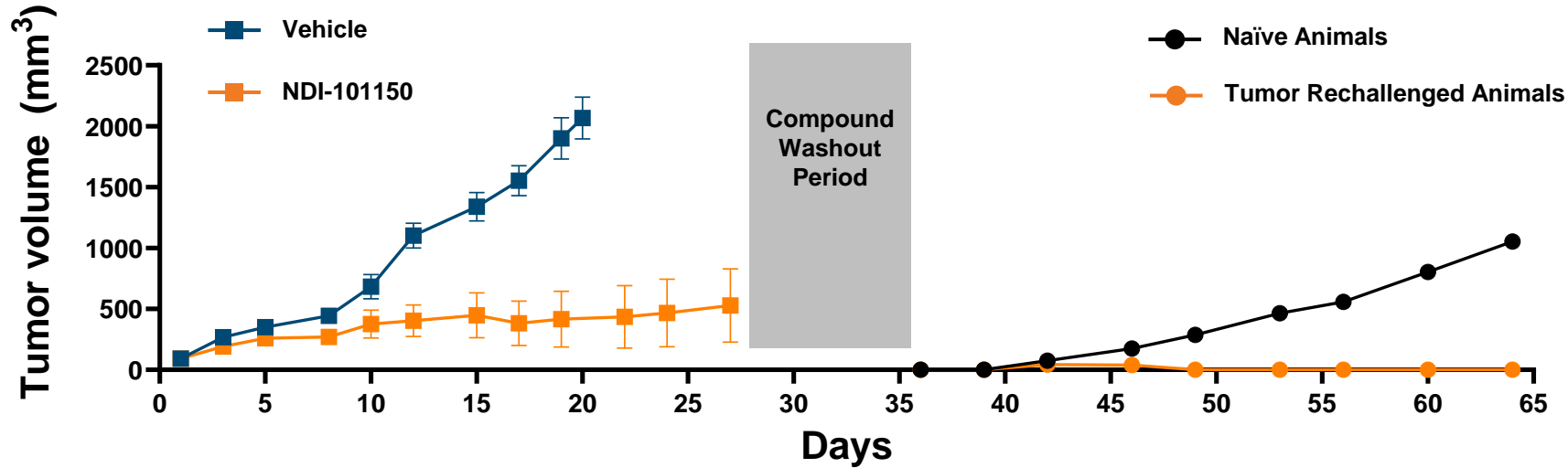


- Enhances IgG secretion by B cells
- Enhances activation and antigen presentation in bone marrow derived dendritic cells

MAP4K = mitogen-activated protein kinase kinase kinase kinase., Treg = regulatory T cells; PGE2 = prostaglandin E2, TGF β = transforming growth factor beta; IgG = immunoglobulin G

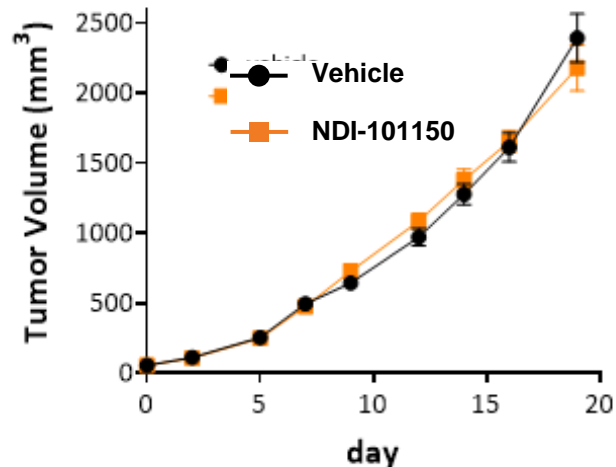
NDI-101150 Demonstrates Robust Efficacy in the EMT-6 Syngeneic Mouse Model, in an Immune-dependent Manner

Robust Efficacy & Durable Immune Memory in the Murine EMT6 Syngeneic Tumor Model

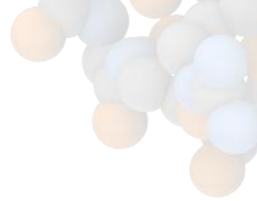


- NDI-101150 75mpk/day, po showed 7 complete responses (CRs) of 10 mice
- After rechallenge with tumor, NDI-101150 cured mice show complete tumor regression **without any further dosing**

No Efficacy Observed in EMT-6 Xenograft Model



- NDI-101150 75mpk/day, po did NOT induce tumor growth inhibition in a xenograft version of EMT6 showing that HPK1 inhibition is mediated through the animals immune system



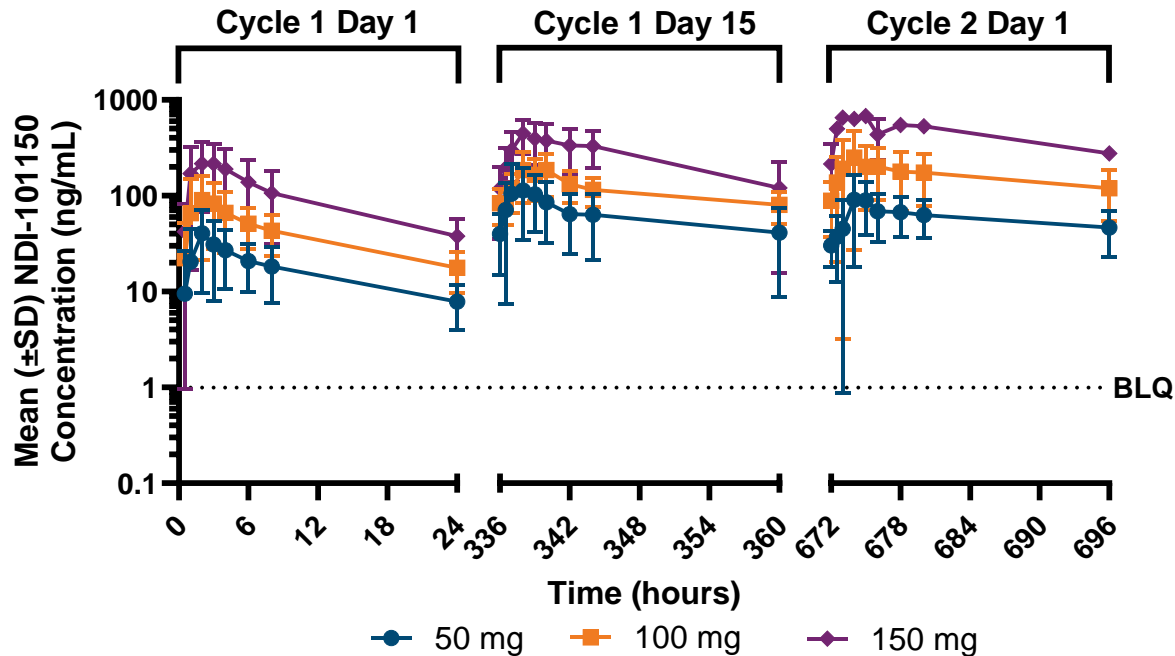
NDI-101150 is being investigated in a Phase 1/2 Clinical Trial

- Phase 1/2 multicenter, open-label trial (NCT05128487) designed to assess NDI-101150 as a monotherapy (50-200 mg dose) and in combination with 200 mg pembrolizumab in the treatment of adults with advanced solid tumors
- Primary objectives: recommended phase 2 dose(s) and maximum tolerated dose
- Secondary objectives: safety, pharmacokinetic profiles, and preliminary antitumor activity
- Preliminary results* presented at the 2024 ASCO Annual Meeting showed:
 - **Data from 44 patients in the dose escalation cohorts** (n=38 on monotherapy, n=6 on combination therapy) and 15 patients in the dose expansion cohorts
 - **NDI-101150 was well-tolerated with overall acceptable safety profile**
 - NDI-101150 plasma concentrations increased in a near dose-proportional manner
 - Steady-state plasma concentrations at all doses were sufficient to cover the pSLP76 IC50 for a duration consistent with preclinical efficacy modeling
 - **NDI-101150 showed an increase in activated CD8+ T cells and dendritic cell infiltration in on-treatment patient biopsies compared to archival biopsies, consistent with nonclinical studies of NDI-101150 showing immune cell infiltration and robust anti-tumor activity in murine syngeneic tumor models**
 - **Treatment with NDI-101150 monotherapy was associated with clinical benefit in five out of 30 (16.7%) response-evaluable patients, including one complete response, one partial response, and three cases of durable stable disease**

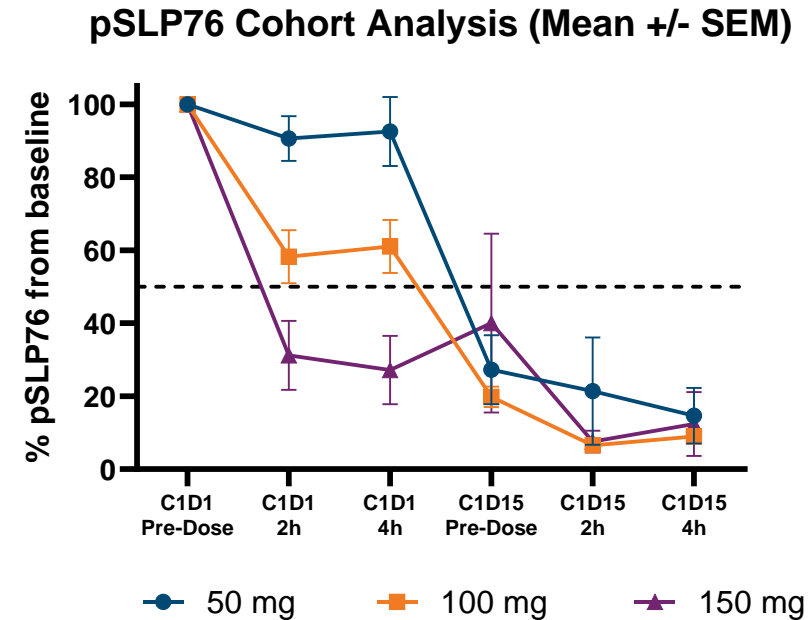
*Data cut-off: March 18, 2024

Preliminary Monotherapy Pharmacodynamic and Pharmacokinetic Results from an Ongoing Phase 1a Dose Escalation Study of NDI-101150

Mean concentration on Cycle 1 Day 1, Day 15 & Cycle 2 Day 1



Change in percentage pSLP76 from baseline to Cycle 1 Day 15



- NDI-101150 showed a dose-dependent increase in plasma concentration and accumulation at steady state, with pSLP76 inhibited at all doses
 - Nearly dose proportional increases in mean exposure was observed on Cycle 1 Day 1
 - Steady state was achieved by Cycle 1 Day 15
 - Accumulation was observed between Cycle 1 and Cycle 2
 - PD results demonstrated >50% reduction of pSLP76 (proposed therapeutic target) in each cohort by Cycle 1 Day 15



Summary

- Knowledge-based hit generation approach was the most successful of four hit generation campaigns
- SBDD applied to optimize both potency and selectivity
 - Multiple proprietary crystal structures of HPK1, GLK and KHS obtained
 - Co-crystal structures of near neighbor kinases applied to optimize selectivity
 - Protein/ligand structures guided SBDD and FEP despite highly flexible protein
 - Off-target undesired activity, e.g. AChE, hERG removed by modeling strategy
- Potent and Selective HPK1 inhibitors were optimized for their predicted human dose
 - Addition of basic groups to inhibitors to improve phys props (\uparrow volume of distribution, \uparrow solubility, \downarrow Cl_{int}) to improve predicted human dose and half life
- NDI-101150 was identified as a potent HPK1 inhibitor which showed
 - High selectivity both within the MAP4K family and in the wider kinome
 - Activation of T cells, B cells and dendritic cells, to mount a robust anti-tumor response
 - Robust preclinical activity, both as a monotherapy and with synergistic efficacy in CPI combinations
- NDI-101150 is currently being investigated in a Phase 1/2 clinical trial (NCT05128487)
 - NDI-101150 treatment associated with activated CD8+ T cells and dendritic cell infiltration in tumors
 - Treatment with NDI-101150 monotherapy resulted in preliminary evidence of clinical benefit and an acceptable safety profile

Acknowledgements



Beth Browning
Samantha Carreiro
David Ciccone
Alan Collis
Scott Edmondson
Abbas Kazimi
Christine Loh
Joshua McElwee
Peter Tummino
Lewis Whitehead

Anita Scheuber
Bhaskar Srivastava
Scott Daigle
Scott Boiko
Amanda Hoerres
Frank G Basile
Xinyan Zhang
Patricia Fraser
Sue Dasan
Daria Chabas
Mark Carlson
Denise Levasseur
Hyesun Oh
Avinash Phadke
Vinayak Hosagrahara
Gabby Poirier
Pavan Kumar
Jeff Conant
Cindy Fung

Steven Albanese
Asela Chandrasinghe
Alexandre Cote
Eric Feyfant
Jeremy Greenwood
Abba Leffler
Dan Severance
Shawn Watts

Anya Avrutskaya
Matthew Benson
Mike Briggs
Bethany Bowers
Thi Bui
Erica Goldsmith
Victoria Hughes
Marieke Lamers
Vad Lazari
Phil Leonard
Ian Linney
Natalie Lyall-Varnas

Sarah L Martin
Anthony Middleton
Nick Pearson
Adam Ringrose
Stuart Ward
Yvonne Walker
Ben Whittaker
Douglas Weitzel
Grant Wishart
Eddie Wood
Benno Van El